Independent Heterologous Fibrillation of Insulin and Its B-Chain Peptide

Dong-Pyo Hong and Anthony L. Fink*

Department of Chemistry and Biochemistry, University of California, Santa Cruz, California 95064

Received August 19, 2005; Revised Manuscript Received October 1, 2005

ABSTRACT: Insulin is very prone to form amyloid fibrils under slightly destabilizing conditions, and the B-chain region plays a critical role in the fibrillation. We show here that the isolated B-chain peptide of bovine insulin also forms fibrils at both acidic and neutral pH. When a mixture of insulin and the B-chain peptide was incubated at either acidic or neutral pH, the formation of fibrils was clearly separated into two phases, with the faster phase corresponding to the formation of homogeneous fibrils from the B-chain and the slower phase corresponding to homogeneous fibrillation of insulin. To further investigate the interaction (or lack thereof) between the two polypeptides, we examined the effects of cross-seeding. The results indicate that seeds of B-chain fibrils accelerate the fibrillation of insulin at pH 1.6 and inhibit the fibrillation at pH 7.5, but seeds of insulin fibrils have little effect on the fibrillation of the B-chain. We conclude that at pH 7.5 simultaneous independent homologous fibrillation occurs, but at low pH, heterologous fibrillation takes place, and with B-chain seeding of insulin, a unique conformation of fibrils is formed. Our results demonstrate that in the co-aggregation of closely related peptides each peptide species may undergo concurrent homogeneous or heterologous polymerization and that fibrils of one species may or may not seed fibrillation of the other. The results demonstrate the significant "species" barrier in amyloid fibril formation between fibrillation induced by different fibrils. A model for the fibrillation of the heterogeneous system of insulin and B-chain insulin is proposed.

In contrast to the more frequently observed disordered (or amorphous) aggregates, some proteins form ordered aggregates, termed amyloid fibrils (*1*−*3*). Although most are related to diseases, it has been shown that several proteins (*4*, *5*), peptides (*6*, *7*), and even poly-amino acids (*8*) that are not related to disease can also form fibrils. Amyloid fibril formation is now recognized as a common phenomenon for many proteins (*9*). No sequence or structural similarity between different precursor proteins has been found, suggesting that there may be many pathways leading to amyloid fibrillation and that the polypeptide backbone is a critical factor (9). Amyloid fibrils are normally homogeneous, and it is rarely possible to form chimeric fibrils composed of distinct amyloid proteins or peptides (*10*−*12*). This high "species barrier" suggests that the amyloid fibrils are stabilized by specific interactions of their component polypeptides, which are governed by the characteristic primary and higher order structures of each amyloid protein. Other reports, however, concerning heterogeneous systems consisting of a protein and a peptide fragment corresponding to its key amyloidogenic region (*13*) or similar peptides (*14*−*17*), have shown that heterologous fibrillation may occur, although with a long lag time. The mechanism of this heterologous fibrillation is still unknown. It is well-established that the kinetics of fibrillation can be significantly accelerated by the addition of seed fibrils, which, at a sufficient concentration (usually 1−10%), will abolish the lag time completely (*18*).

* To whom correspondence should be addressed: Department of Chemistry and Biochemistry, University of California, Santa Cruz, CA 95064. Telephone: (831) 459-2744. Fax: (831) 459-2935. E-mail: enzyme@ucsc.edu.

Insulin is a small protein hormone that is crucial for the control of glucose metabolism and in diabetes treatment. It is composed of two polypeptide chains, the A-chain (21 residues) and the B-chain (30 residues) linked together by two disulfide bonds (*19*, *20*) (Figure 1). In solution, insulin exists as an equilibrium mixture of monomers, dimers, tetramers, hexamers, and possibly higher associated states, depending upon the concentration, pH, metal ions, ionic strength, and solvent composition (*21*). Insulin is susceptible to fibril formation on exposure to elevated temperatures, low pH, organic solvents, and agitation (*4*, *22*−*35*). Although there have been several studies investigating the underlying molecular basis of insulin fibrillation, the molecular mechanism or pathway of the fibrillation is still not fully understood. When fibrils of insulin are grown in aqueous solution or 20% ethanol at pH 1.9, their IR spectra are slightly different, reflecting different fibril morphologies. These morphologies "breed" true in the sense that seeds grown under one set of conditions but added to soluble insulin under the other set of conditions have the morphology of the seed fibrils (*27*). This is probably a general feature of fibril seeding (*36*).

For many proteins that form amyloid fibrils, fibril formation is facilitated by amino acid mutations that destabilize the native state. However, insulin is amyloidogenic in the wild-type form. Although no *in vivo* amyloidogenic mutation has been described, Brange and co-workers (*4*, *37*, *38*) showed that the propensity for fibril formation increases with increasing truncation of the C-terminal region of the B-chain, indicating the significance of the B-chain in insulin fibrillation. Using insulin mutants, we have previously shown that a region in the B-chain is critical in the intermolecular association events that lead to insulin fibril formation (*39*).

10.1021/bi051658y CCC: $30.25
Published on Web 11/24/2005

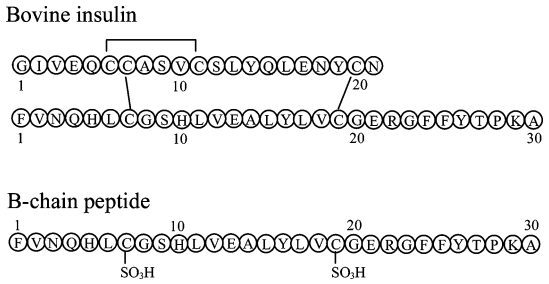

FIGURE 1: Primary structure of bovine insulin (top) and its B-chain peptide (bottom). In the B-chain peptide, the Cys side chains have been oxidized to prevent disulfide formation.

In this study, we focused on fibrillation in a mixture of bovine insulin and its B-chain peptide (Figure 1). Our results show that mixtures of the two peptides form fibrils in distinctly separate processes and do not interact to form heterologous fibrils.

MATERIALS AND METHODS

Materials. Monocomponent bovine insulin (batch 9601331) was obtained from Novo Nordisk A/S, Denmark. The zinc content was 0.4% (w/w of insulin), corresponding to approximately 2 Zn^{2+}/insulin hexamer. The B-chain of bovine insulin was purchased from Sigma, St. Louis, MO, and the thiol groups of the cysteine residues were oxidized to the sulfonic acid (Figure 1). Both intact insulin and the B-chain were homogeneous, as judged by the single band visible on SDS−PAGE gels stained with Coomassie Blue. Thioflavin T (ThT)[1] was obtained from Fluka.

Preparation of Insulin Samples. All protein samples were prepared immediately prior to the kinetics experiments. Insulin and the B-chain peptide were dissolved at a concentration of 2 mg/mL in the appropriate buffer. The insulin concentration measured at 276 nm using an extinction coefficient of $A = 1.08$ for 1.0 mg/mL (*40*). The extinction coefficient (ϵ) for the B-chain was calculated from its amino acid sequence (*41*). Fibril formation was studied in two different media: 50 mM phosphate buffer and 100 mM NaCl at pH 7.5, and 25 mM HCl and 100 mM NaCl at pH 1.6, using 2 mg/mL polypeptide.

ThT Fluorescence Assays for Fibrillation. A stock solution of ThT was prepared at a concentration of 1 mM in distilled water and stored at 4 °C, protected from light to prevent photooxidation. For *in situ* ThT fluorescence measurements, 10 μM ThT was added to each of the protein solutions to be incubated in a 96-well plate; A 100 μL sample volume was added to each well. Five replicates corresponding to five wells were measured for each sample to minimize the well−well variation. The plate was covered by Mylar plate sealer and incubated at 37 °C with shaking. The agitation was continuous except for readings at 15 min intervals, and the speed of the agitation was 600 rpm with a shaking diameter of 1 mm. The fluorescence measurements were performed on a fluorescence plate reader (Fluoroskan Ascent). The fluorescence was measured with an excitation at 450 nm and emission at 485 nm and curve-fit as described in ref *39*.

After fibrillation was complete, the samples of the fibril solution were centrifuged at 14 000 rpm for 30 min and the protein and ThT concentrations in the supernatant solutions were measured with a Shimadzu UV spectrophotometer, model UV-2401PC.

ATR−FTIR Spectroscopy. Attenuated total reflectance Fourier transform infrared (ATR−FTIR) spectra were recorded on a ThermoNicolet Nexus 670 FTIR spectrometer equipped with an MCT detector. The samples were prepared as hydrated thin films as previously described (*42*, *43*) on the surface of an out-of-compartment germanium trapezoidal internal reflectance element (IRE). A total of 512 interferograms were co-added at 1 cm^{-1} resolution to generate each spectrum. Spectra were deconvoluted to ascertain the percents of secondary structure using GRAMS32 (Galactic Industries). Fourier self-deconvolution (FSD) and second derivatives were used to deconvolve the spectra. Peak positions identified by both were used for the curve-fitting routine. In curve fitting, the initial peak positions found were fixed and the peak width was allowed to vary from 15 to 30 cm^{-1}. The peak height, width, and percent Lorentzian were allowed to vary until the solution converged to a minimum, at which time the constraint on the peak positions was removed and curve-fitting continued until the minimum was reached. Percent secondary structure peak assignments were made as previously published (*42*, *43*).

Cross-Seeding Experiments. Sonicated fibrils of insulin and B-chain peptide were used as seeds in cross-seeding experiments. Seeds were prepared as follows: a solution of fibrils (2 mg/mL) was centrifuged at 14 000 rpm for 30 min. After the supernatant was removed, the pellet was suspended in water, and mildly sonicated. As desired, the sonicated seed fibrils were short, 50−300 nm, on the basis of electron microscopy (EM) images. The effect of cross-seeding on the kinetics of fibrillation was studied by adding 10% (w/w) of the seeds.

Electron Microscopy. Transmission electron micrographs were collected using a JEOL JEM-100B microscope operating with an accelerating voltage of 80 kV. Typical nominal magnifications ranged from 30 000 to 75 000×. Samples were deposited on Formvar-coated 300-mesh copper grids and negatively stained with 1% aqueous uranyl acetate.

RESULTS

Amyloid Fibril Formation. The time course of the fibrillation of insulin and its B-chain peptide during incubation was monitored using ThT fluorescence (parts A and B of Figure 2). ThT is a widely used fluorescence dye, whose fluorescence emission increases substantially upon binding to amyloid fibrils. Fluorescent measurements were carried out every 15 min for approximately 80 h at 37 °C. Although the lag times of the B-chain peptide fibril formation were not markedly dependent upon the pH, insulin fibrillation was substantially faster at pH 1.6 than at pH 7.5. This is due to the fact that conditions of low pH favor mono- or dimeric insulin, whereas neutral pH conditions favor tetramer or hexamer (*39*, *44*). It has been shown that dissociation of insulin hexamers is the rate-limiting step in fibrillation at neutral pH and that the active fibrillating species is the monomer (*25*, *30*). In addition, very different maximal ThT signals were observed for insulin and B-chain, although the amount of fibrils formed was almost the same (95% of total protein) at all pH values, on the basis of the concentration

[1] Abbreviations: ThT, thioflavin T; EM, electron microscopy.

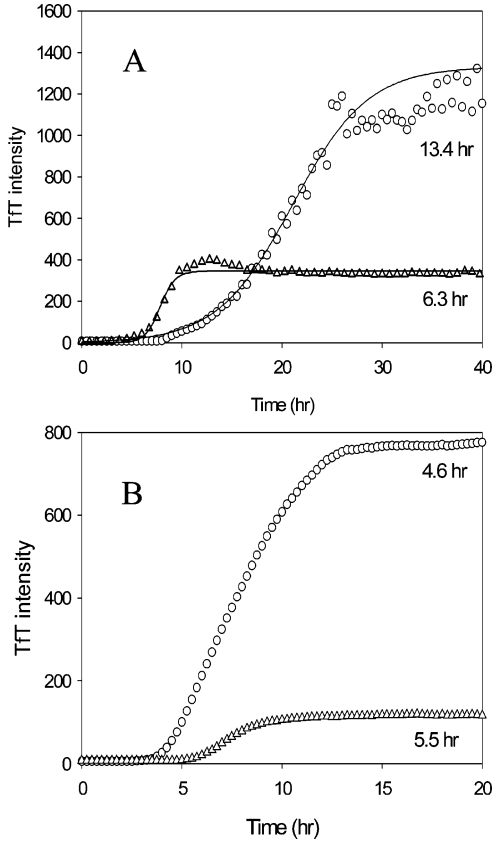

FIGURE 2: Kinetics of fibril formation of bovine insulin and its B-chain peptide at (A) pH 7.5 and (B) pH 1.6: insulin (○) and B-chain peptide (△). Fibril formation was monitored by ThT fluorescence. The numbers shown indicate the lag times of each fibrillation. The concentration of B-chain and insulin were 2 mg/mL protein.

of protein in the supernatant and pellet (see the Materials and Methods). Many factors can affect the ThT signal intensity: in this case, we believe it reflects differences in the structure/morphology of the insulin and B-chain fibrils. Support for this comes from the analysis of the FTIR spectra of the fibrils from insulin and B-chain (parts A and B of Figure 3), which show significant differences in the amide I region, corresponding to the secondary structure. For example, not only are the β-sheet component bands centered at different frequencies, but also the fraction of β-sheet is different, namely, 60% for the B-chain peptide and 66% for insulin (Table 1). These spectra are for fibrils grown at pH 1.6, but the corresponding spectra for fibrils grown at pH 7.5 were essentially identical to those at pH 1.6. Components in the amide I region in the vicinity of 1640−1620 cm^{-1} are usually ascribed to β-sheet or extended structure (the spectra in Figure 3 are in H_2O). Components in the mid-1650's are attributed to helices, and at slightly lower frequencies, they are attributed to the disordered structure. Bands in the high 1650's and 1660's usually arise from loops, and most of the higher frequency components are from turns (*45*). Thus, the major changes in the secondary structure between fibrils of insulin and the B-chain involve β-structure and loops.

The formation of fibrils by the B-chain was confirmed by EM (Figure 4). The straight fibrils, with a diameter of 7−12 nm and a longitudinal periodicity of 27−30 nm, were similar to those of insulin (diameter of 8−12 nm). In fact, the fibrils of the B-chain and insulin are almost indistinguishable by EM, although the B-chain fibrils are shorter at pH 7.5.

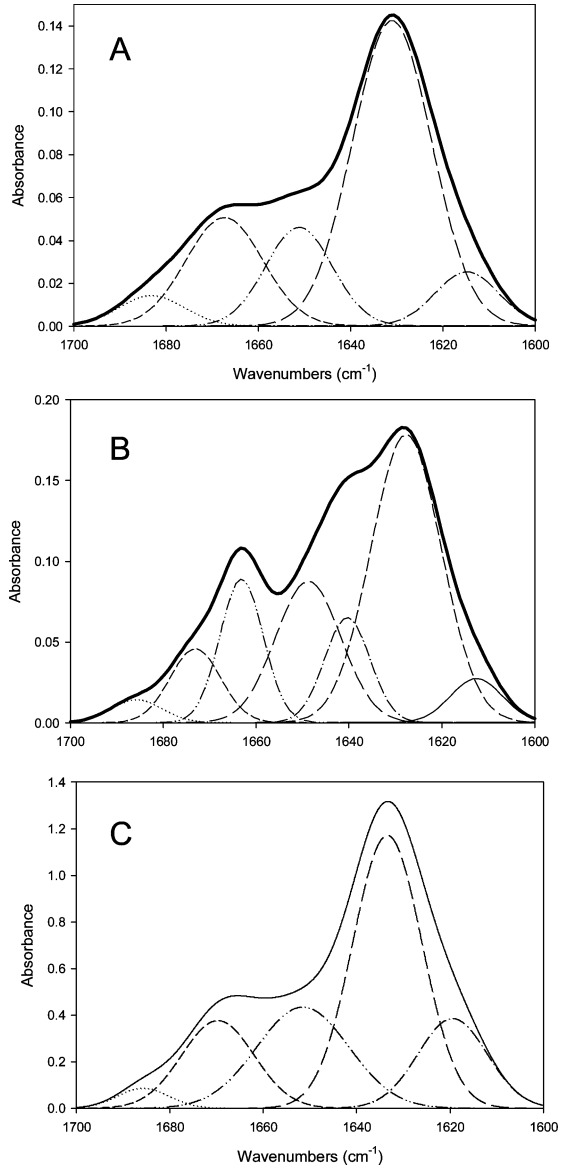

FIGURE 3: FTIR spectra of insulin and B-chain fibrils show differences in underlying secondary structure. A shows the amide I region for insulin fibrils; B is for B-chain fibrils; and C is for insulin fibrils seeded with B-chain, all at pH 1.6. The dashed traces are the curve-fit components following deconvolution (see the text) corresponding to the different secondary structures. Secondary structure composition is given in Table 1.

Table 1: Secondary Structure Differences in Fibrils of Insulin, B-Chain, and B-Chain-Seeded Insulin[a]

	insulin fibrils		B-chain fibrils		insulin fibrils, seeded with B-chain	
assignment	peak (cm^{-1})	area (%)	peak (cm^{-1})	area (%)	peak (cm^{-1})	area (%)
β	1683	4.7	1686	2.6	1686	2.5
turn	1667	18.8	1673	7.9	1670	15.2
loop			1663	13.1		
disordered	1650	14.9	1649	19.2	1651	22.3
β/extended			1640	10.1		
β/extended	1630	53.7	1628	42.1	1633	45.3
side chain/β/extended	1615	7.8	1612	4.9	1620	14.8

[a] The errors in percent secondary structure are 10−15%.

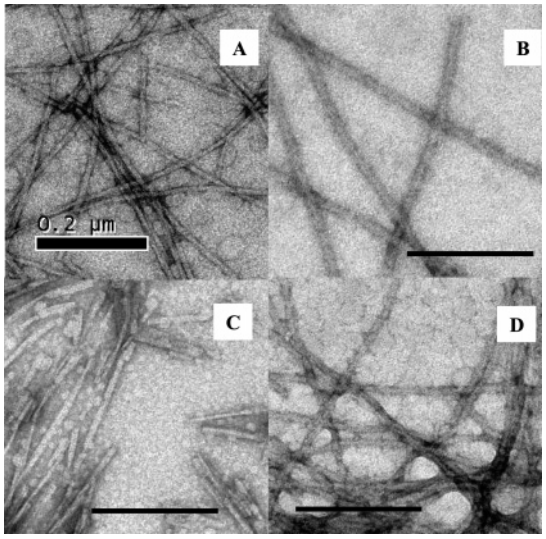

FIGURE 4: Negative-staining transmission electron micrographs of bovine insulin and B-chain fibrils. Insulin fibrils were grown at pH 7.5 (A) and pH 1.6 (B). B-Chain fibrils at pH 7.5 (C) and pH 1.6 (D). Scale bars are 200 nm.

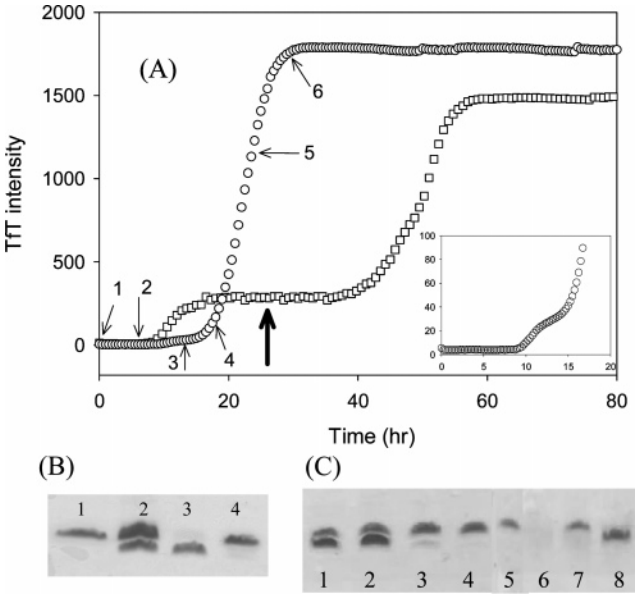

FIGURE 5: Fibril formation from a 1:1 mixture of insulin/B-chain peptide. (A) Kinetics of fibrillation monitored by ThT for the mixture at pH 7.5 (□) and pH 1.6 (○). The inset shows the data of pH 1.6 magnified between 0 and 20 h. (B) SDS−PAGE gel analysis of the supernatant and pellet of samples taken at 24 h from the mixture at pH 7.5 (indicated by the bold arrow). Lane 1, insulin alone; lane 2, mixture of insulin and B-chain; lane 3, pellet from the mixture; and lane 4, supernatant from the mixture. (C) SDS−PAGE gel analysis of supernatants of samples taken as a function of time from the mixture incubated at pH 1.6 [indicated by the fine arrows; 0 h (1), 7 h (2), 13 h (3), 17 h (4), 23 h (5), and 30 h (6)]. The lanes on the gel correspond to the sample numbers, and lanes 7 and 8 are insulin alone and B-chain alone, respectively.

Fibril Formation in Mixtures of Insulin and B-Chain. The fibrillation of 1:1 mixtures of insulin/B-chain were examined at acidic and neutral pH (Figure 5A). At pH 7.5, the results show two completely separate fibrillation curves of different amplitude, suggesting the presence of independent fibrillation by the two peptides. ThT is known to bind rapidly to amyloid fibrils accompanied by an increase of fluorescence. The observed double-transition curve, therefore, is most simply interpreted as corresponding to the fibrillation of two independent species with different kinetics. This was confirmed as follows: after completion of the first transition, we separated the pellet and supernatant fraction by centrifugation and ran SDS−PAGE on the samples (Figure 5B). The pellet fraction had a band at the position of the B-chain on the gel, and the supernatant fraction showed a band corresponding to insulin. These results demonstrate that insulin and B-chain peptide form fibrils independently and at different rates. The first transition corresponds to formation of B-chain fibrils, and the second transition corresponds to insulin fibril formation. The lag times of each fibrillation, however, were significantly increased when compared to those of each alone (2-fold for the B-chain and 3-fold for insulin), as shown in Figure 2, indicating that the presence of the second fibrillating system resulted in some inhibition of nucleation.

Although the fibrillation of the mixture at pH 1.6 seems to be a single-transition curve (Figure 5A, ○), in fact, it is the superposition of two nearly simultaneous independent fibrillations (which, in fact, can be seen in the blow-up of the data in the inset to Figure 5A). This was demonstrated using SDS−PAGE analysis of the supernatants of samples taken as a function of time (Figure 5C). The results show that the band corresponding to the B-chain peptide disappears initially, followed by that of the insulin, indicating that the first transition is due to fibrillation of the B-chain peptide. Although the lag time for insulin alone is shorter than that of the B-chain alone (see Figure 2), the fibrillation of insulin occurred immediately after B-chain fibrillation in the mixture at pH 1.6, in contrast to the result at pH 7.5. These results indicate that the fibrillation of insulin is significantly inhibited by the B-chain peptide at both pH values; however, the presence of insulin in the mixture has little effect on the fibrillation of the B-chain. Similar data were obtained using different ratios of the B-chain/insulin concentration (1:2 and 2:1) at pH 1.6, with an initial small increase of the ThT signal followed by a second larger amplitude transition, confirming that the second fibrillation (that of insulin) is affected by the B-chain fibrillation (data not shown). Another point of interest is that the maximum fluorescent intensity of ThT in the heterogeneous fibrillation at pH 1.6 was higher than the predicted value (on the basis of the sum of the individual intensities), although at pH 7.5, they showed the predicted value. The reason for this high fluorescence intensity is unclear but is probably due to the fibrillation of the insulin, because the contribution of the B-chain signal is very small (see the inset of Figure 5A) and probably reflects small changes in the fibril structure that affect the local environment of bound ThT, although other explanations are possible.

Cross-Seeding between Insulin and B-Chain Peptide. To obtain insight into the mechanism of fibril formation in the heterogeneous system, we examined cross-seeding between B-chain and insulin (Figure 6). Although insulin at pH 1.6 forms amyloid fibrils with a lag time of several hours, the addition of seeds composed of sonicated insulin fibrils accelerates the rate substantially and abolished the lag (Figure 6A), indicating that the insulin fibrils worked directly as seeds in the fibrillation of insulin. The magnitude of the final ThT signal was almost the same as that in the absence of seeds. Intriguingly, upon the addition of seeds of the B-chain fibrils, the fibrillation of insulin was also accelerated,

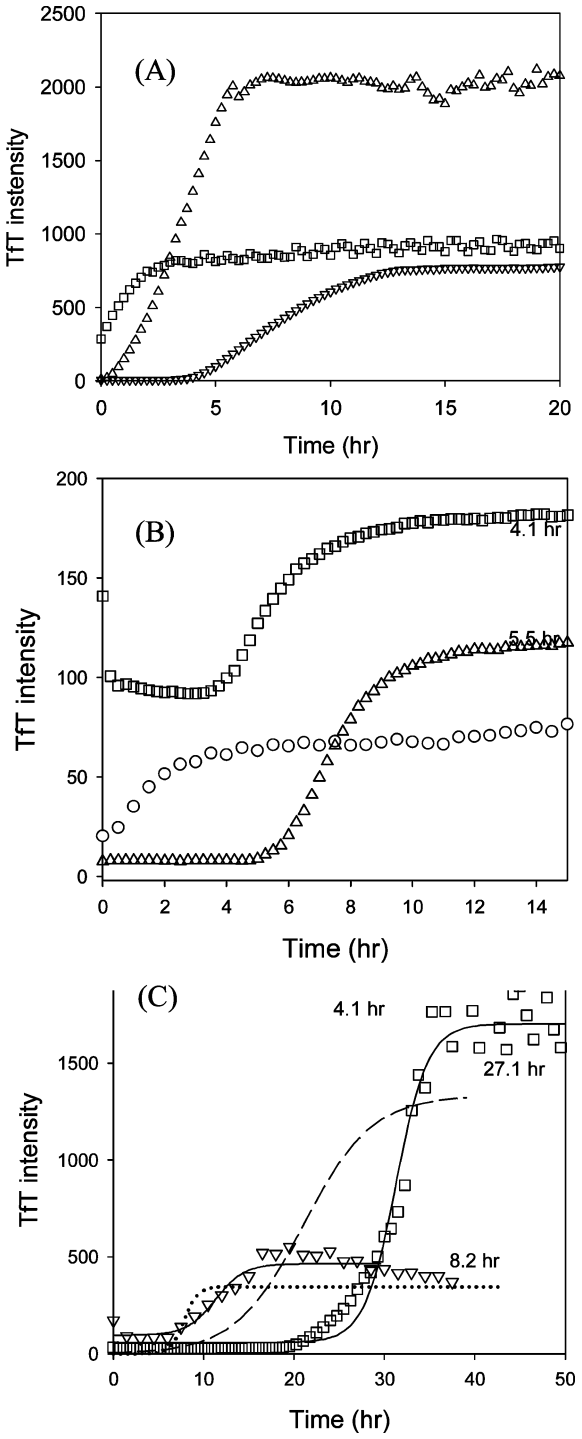

FIGURE 6: Influence of seeding on the kinetics of bovine insulin fibrillation. (A) Effect of seeding on insulin fibrillation at pH 1.6: (▽) insulin alone (2 mg/mL), (□) 10% insulin fibril seeds added, and (△) 10% B-chain fibril seeds added. (B) Effect of seeding on the fibrillation of B-chain peptide (2 mg/mL) at pH 1.6: (△) B-chain alone), (○) 10% B-chain fibril seeds added, and (□) 10% insulin fibril seeds added. (C) Effect of cross-seeding at pH 7.5: (□) insulin fibrillation in the presence of 10% B-chain fibrils and (▽) B-chain fibrillation in the presence of insulin fibrils. The values indicate the lag times of each fibrillation. The dotted line represents fibrillation of B-chain without seeding, and the dashed line represents fibrillation of insulin alone.

suggesting that the growing face of B-chain fibrils may resemble that in insulin fibrillation. The lag time in this case was very short but detectable; interestingly, the final ThT intensity was significantly larger than with insulin alone

Table 2: Summary of the Effect of pH and Cross-Seeding on the Lag Time for Insulin and B-Chain Fibrillation[a]

fibrillation experiments			cross-seeding experiments	
insulin	pH 1.6	4.6 (±0.5)	10% B-chain fibrils	<0.2
	pH 7.5	13.4 (±1.2)		27.1 (±2.4)
B-chain	pH 1.6	5.5 (±0.2)	10% insulin fibrils	4.1 (±0.6)
	pH 7.5	6.3 (±0.4))		8.2 (±0.5)
mixture of insulin and B-chain	pH 1.6	insulin	14.0 (±0.3)	
		B-chain	9.2 (±0.4)	
	pH 7.5	insulin	38.0 (±7.0)	
		B-chain	9.7.0 (±1.1)	

[a] The numbers refer to the lag time in hours, and the standard deviations are given in parentheses.

(Figure 6A). On the other hand, in the opposite experiment, there was little effect of cross-seeding with seeds from insulin on the fibrillation of the B-chain peptide at pH 1.6 (Figure 6B; the higher initial ThT reading is due to the signal from the added seeds). Cross-seeding experiments at pH 7.5 showed no acceleration of fibrillation by the hetero seeds (Figure 6C); in fact, fibrillation of insulin was significantly inhibited by the presence of seeds of the B-chain. This observation is consistent with the result that fibrillation of insulin is significantly inhibited by the B-chain fibrils in the mixture at pH 7.5 (Figure 5A). Table 2 summarizes the results for the lag time for the various conditions used.

DISCUSSION

Our previous results demonstrated that a region in the B-chain is important for insulin fibril formation (*34*). The current study focused on fibrillation of the B-chain peptide and mixtures of insulin and B-chain peptide. Insulin exists predominantly as the hexamer in the presence of zinc at neutral pH and predominantly as the dimer at pH 1.6 (*4*, *39*, *44*). It has been proposed that insulin fibrillation occurs through the dissociation of oligomers into the monomer and that the monomer undergoes a structural change to a partially folded conformation having a strong propensity for fibrillation (*4*, *39*, *44*, *46*−*48*). The fibrillation of the insulin B-chain peptide is relatively independent of pH, presumably because, unlike insulin itself, there is no pH-dependent oligomer (e.g., hexamer) dissociation involved. In addition, the rate of insulin fibrillation is almost the same as that of the B-chain at low pH, where insulin is mostly present as a dimer (with some monomer), suggesting that they have similar potential for fibrillation under these conditions. The intensity of the ThT fluorescence of the B-chain fibrils at the same concentration (by weight) was much less than that of the insulin fibrils, suggesting differences in the structure of the fibrils, which was confirmed by the differences in the FTIR spectra. Many characteristics of amyloid fibrils, such as staining properties with Congo red or ThT, fibrillar structure from EM, and cross-β-sheet structure, are common to amyloid fibrils formed from different polypeptides. To understand the mechanism of amyloid fibril formation, it is important to know the basis for the common properties as well as their differences. Experiments involving the fibrillation of heterologous systems and cross-seeding provide information regarding their differences.

Amyloid fibril formation is usually considered to be a nucleation-dependent process in which monomers occasionally associate to form the nuclei. This nucleation process

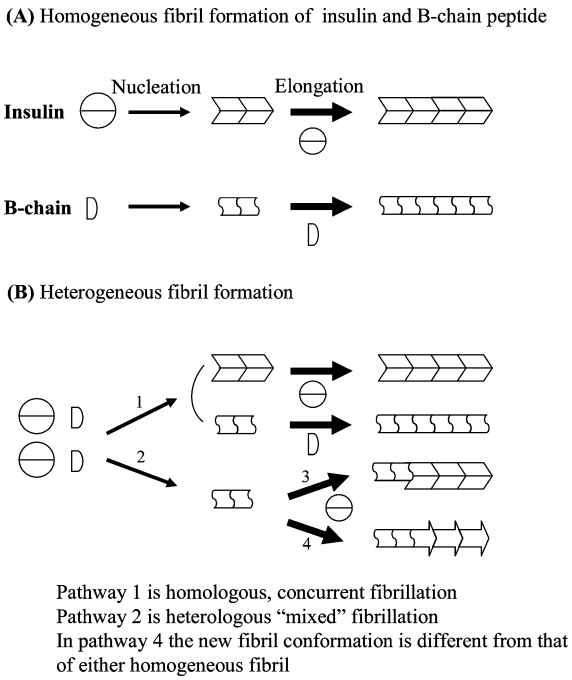

FIGURE 7: Schematic representation of the mechanisms of homogeneous fibril formation of bovine insulin and B-chain peptide (A) and heterogeneous amyloid fibril formation of bovine insulin and B-chain (B). Pathway 1, homologous independent fibrillation in the heterogeneous system; pathway 2, heterologous fibrillation in which fibrils from first fibrillation induce fibrillation in the second; pathway 3, formation of the "normal" type of insulin fibril structure as formed in the homogeneous system to the B-chain seeds; and pathway 4, formation of a different type of insulin fibril structure, which could be similar to that for B-chain or different from both that of homogeneous insulin or B-chain.

requires a series of association steps, which are thermodynamically unfavorable, and represent the rate-limiting step in amyloid fibril formation *in vitro*. Once the nucleus has been formed, further addition of monomers becomes thermodynamically favorable, resulting in rapid extension of the fibril, which grows by sequential incorporation of more monomer protein onto the ends of the growing fibrils.

The results of heterogeneous fibrillation and cross-seeding experiments between insulin and B-chain peptide can be explained on the basis of the schematic mechanisms outlined in Figure 7. The fibrillation of both insulin and B-chain individually form homogeneous fibrils. However, in a heterogeneous mixture of insulin and B-chain peptide, two major possibilities exist: either independent fibrillation of each polypeptide, i.e., two concurrent homologous fibrillations (pathway 1 in Figure 7B), or a single heterologous fibrillation where both monomers are incorporated into the same fibrils (pathway 2 in Figure 7B). The latter can occur via more than one mechanism (pathways 3 or 4 in Figure 7B).

Our results for the fibrillation of a mixture of soluble insulin and B-chain peptide at pH 7.5 (Figure 5A) suggest, at first glance, that it conforms to the former model (pathway 1 in Figure 7B). The kinetics of fibrillation of this mixture clearly shows two well-separated fibrillation processes, which correspond to the initial fibrillation of the B-chain, with relatively similar kinetics to fibrillation of the B-chain alone, followed by fibrillation of insulin, but with much slower kinetics than for insulin alone. These much slower kinetics can be explained either by interactions of soluble insulin with fibrils of the B-chain (pathway 1, independent, heterologous fibrillation) or by an alternate pathway, such as that shown in pathways 3 or 4 in Figure 7B. When soluble insulin is seeded with B-chain fibrils at pH 7.5, very slow kinetics are observed, consistent with the results from the mixed soluble polypeptides, although with seeding, the kinetics are not as slow, probably reflecting the time necessary for B-chain fibrils to form in the nonseeded case. The interesting aspect of both of these experiments is that the presence of the B-chain seeds inhibits the rate of insulin fibrillation. This means that there must be significant interactions between soluble insulin and B-chain seeds. Because the rate of fibril *elongation* for soluble insulin is not significantly affected by the presence of the B-chain seeds, it does not allow discrimination between the two pathways. The fact that the nucleation kinetics are much slower than in the absence of the B-chain seeds suggests two possibilities: one is that most of the soluble insulin is tied up with the seeds, but homologous fibrillation occurs, with a longer lag time because of the effectively decreased concentration of insulin monomers as a result of their interaction with the seeds (presumably the interaction is not sufficiently complementary to lead to deposition of insulin molecules on the B-chain fibrils but strong enough to transiently tie up some of the insulin); or two, pathway 2 (Figure 7B), in which the initial addition of insulin monomer(s) to the B-chain seeds is slow because of the lack of good complementarity. In addition, increasing the concentration of B-chain seeds leads to longer lag times (data not shown), which is consistent with pathway 1. Because the amplitude of the ThT signal is that expected for the sum of the individual contributions, we believe that at pH 7.5 the mixture of insulin and B-chain follows pathway 1 in Figure 7, i.e., independent homologous fibrillation. The kinetics of fibrillation of soluble B-chain in the presence of insulin seeds shows a negligible effect of the seeds, suggesting no interactions between the soluble peptide and fibrils and again the mechanism of pathway 1.

In contrast to the case at pH 7.5, fibrillation of the mixture of soluble insulin and B-chain seeds at pH 1.6 is most consistent with a model for heterologous fibrillation as shown in pathway 2 in Figure 7B. When soluble insulin and B-chain were incubated at pH 1.6, the B-chain formed fibrils relatively quickly. The resulting seeds of B-chain fibrils then induced fibrillation of insulin, as also observed in the cross-seeding experiments (Figure 6A). This result is very similar to the cross-seeding reactions between β2-microglobulin (β2-m) and its peptide fragment, Ser20−Lys41 (peptide K3), reported by Kozhukh et al. (14). They examined the heterogeneous fibrillation of β2-m and the K3 peptide. Fibrils of K3 peptide induced fibril formation of β2-m. The authors assumed that the K3 peptide constitutes the essential region for β2-m-related amyloid fibril formation, although various other regions have also been shown to be critical (*49*−*51*). As noted, previous data suggest that the B-chain peptide may contain the essential amyloidogenic region for insulin fibrillation; this is supported by the fact that we do not observe any accelerating effect of the A-chain peptide of bovine insulin on the fibrillation of insulin (Hong and Fink, manuscript in preparation). These results suggest that the B-chain fibrils at pH 1.6 may either play a role as a template for insulin fibrillation or accelerate the nucleation of insulin. Conversely, the B-chain region may be buried in fibrils of

insulin so that insulin fibrils do not have much effect on the fibrillation of the B-chain. We also obtained similar results in a mixture of insulin (2 mg/mL) and B-chain peptide (1 mg/mL) at pH 1.6, indicating that the insulin fibrillation was dependent upon the B-chain fibrillation, although the B-chain fibrillation was slow because of its low concentration (data not shown).

The data of Figure 6A clearly show that B-chain seeds accelerate the fibrillation of soluble insulin by acting as seeds for insulin polymerization. There are two possible explanations: one is that, after a certain number of the monomers of insulin have polymerized onto the ends of the fibrils of the B-chain, the ends would become similar to those of fibrils of insulin (pathway 3 in Figure 7B), as described by Kozhukh et al. (*14*) for β2-m. The other is that the binding of the heteromonomer leads to a different type of fibril from either type of homofibril (pathway 4 in Figure 7B). Support for the latter hypothesis comes from the high ThT fluorescence intensity of the heterogeneous fibrils (Figure 5A; predicted intensity = 900, observed intensity = 1900) and the fibrils formed by seeding insulin with B-chain fibrils (Figure 6A). Because the ThT intensity reflects underlying structural properties of the fibrils, the substantially larger ThT signals of fibrils formed by insulin in the presence of the B-chain at pH 1.6 strongly argue for pathway 4, namely, heterologous fibrillation with a new conformation for the insulin in the elongated fibrils. This is further supported by the relative similarity in FTIR spectra of the fibrils from insulin fibrils grown in the presence of B-chain seeds to those of insulin itself (Figure 3A) and their marked difference from those of B-chain fibrils (Figure 3B). Although the spectra of these fibrils are similar to those of insulin, they are not the same (Figure 3C), which indicates that the underlying secondary structure of the insulin-seeded B-chain fibrils is somewhat different from that in insulin fibrils and quite different from B-chain fibrils. This was quantitated via deconvolution and curve fitting, to yield the secondary structure composition shown in Table 1, which indicates that the amount of β-structure is slightly less in the heterologous fibrils compared to insulin fibrils and that the distribution of β-structure components is also slightly different. The EM images of insulin fibrils and those grown from insulin seeded by the B-chain do not reveal any differences (data not shown).

In contrast to the marked effect of B-chain fibril seeds on insulin fibrillation, insulin seeds had a negligible effect on the fibrillation of the B-chain (perhaps a small acceleration in kinetics) at pH 1.6, suggesting no interaction of soluble B-chain with the insulin seeds, and that insulin seeds do not play a role as a template for B-chain fibrillation, as observed at pH 7.5. This suggests that the growing ends of insulin fibrils do not involve just the B-chain component, whereas for fibrils of the B-chain, the growing ends necessarily involve the B-chain and thus potential complementarity for templating soluble insulin. The heterologous fibrillation for insulin with seeds of the B-chain at pH 7.5 is much slower than at pH 1.6, probably because the insulin is predominantly in the form of the hexamer and most likely has to be monomeric to interact with the B-chain seeds.

These results not only confirm the fact that fibrils are normally homogeneous, highly ordered structures, formed by specific interactions between the growing fibril and the monomer, but also suggest the possibility of formation of heterologous fibrils under some circumstances in which fibrils of similar underlying structure are present. Therefore, we conclude that not only can the monomer of one species inhibit fibrillation of the other but also that the first-formed fibrils may seed fibrillation of the other protein under some conditions. Our results are consistent with those for the fibrillation of hen lysozyme at low pH and high temperature, which can be seeded by fibrils of very similar proteins but not more distantly related ones (*12*), and those of Hasegawa et al. (*13*), who examined homogeneous and heterologous extensions with the Alzheimer's β-amyloid (Aβ) peptides, Aβ-(1−42) and Aβ-(1−40). When the species used for seeds was the same as the species of monomers, they observed no lag phase. In contrast, when the two species were different, a lag phase was observed; similar data have been reported by O'Nuallain et al. (*52*). This behavior is similar to that observed with insulin and B-chain peptide; however, the insulin system also exhibits more complex behavior, demonstrating homogeneous fibrillation at pH 7.5 and heterologous fibrillation at low pH, leading to a unique fibril morphology. There have been a few reports of seeding by unrelated proteins: e.g., fibrils of silk and Sup35 led to deposits of serum amyloid protein (SAA) fibrils (*53*); seeds of Gln/Asn-rich polypeptides promoted Sup35 prion domain fibrillation (*54*); and cross-seeding of the prion protein by seeds from different species (*55*); however, no evidence was presented that the resulting fibril differed from the corresponding homogeneous fibrils.

In conclusion, we report a unique and unambiguous system of heterogeneous fibrillation, leading to both homologous and heterologous fibrillation. Our results indicate that amyloid fibril formation is normally homogeneous with the association of the monomers to growing homologous fibrils; however, under certain conditions, the presence of fibrils from one polypeptide may affect fibrillation of a similar but different polypeptide.

REFERENCES

1. Koo, E. H., Lansbury, P. T., Jr., and Kelly, J. W. (1999) Amyloid diseases: Abnormal protein aggregation in neurodegeneration, *Proc. Natl. Acad. Sci. U.S.A. 96*, 9989−9990.
2. Kelly, J. W. (1998) The alternative conformations of amyloidogenic proteins and their multi-step assembly pathways, *Curr. Opin. Struct. Biol. 8*, 101−106.
3. Gillmore, J. D., Hawkins, P. N., and Pepys, M. B. (1997) Amyloidosis: A review of recent diagnostic and therapeutic developments, *Br. J. Haematol. 99*, 245−256.
4. Brange, J., Andersen, L., Laursen, E. D., Meyn, G., and Rasmussen, E. (1997) Toward understanding insulin fibrillation, *J. Pharm. Sci. 86*, 517−525.
5. Guijarro, J. I., Sunde, M., Jones, J. A., Campbell, I. D., and Dobson, C. M. (1998) Amyloid fibril formation by an SH3 domain, *Proc. Natl. Acad. Sci. U.S.A. 95*, 4224−4228.
6. Ohnishi, S., Koide, A., and Koide, S. (2000) Solution conformation and amyloid-like fibril formation of a polar peptide derived from a β-hairpin in the OspA single-layer β-sheet, *J. Mol. Biol. 301*, 477−489.
7. MacPhee, C. E., and Dobson, C. M. (2000) Chemical dissection and reassembly of amyloid fibrils formed by a peptide fragment of transthyretin, *J. Mol. Biol. 297*, 1203−1215.
8. Fandrich, M., and Dobson, C. M. (2002) The behaviour of polyamino acids reveals an inverse side chain effect in amyloid structure formation, *EMBO J. 21*, 5682−5690.
9. Dobson, C. M. (2004) Principles of protein folding, misfolding, and aggregation, *Semin. Cell Dev. Biol. 15*, 3−16.
10. Santoso, A., Chien, P., Osherovich, L. Z., and Weissman, J. S. (2000) Molecular basis of a yeast prion species barrier, *Cell 100*, 277−288.

11. Chien, P., and Weissman, J. S. (2001) Conformational diversity in a yeast prion dictates its seeding specificity, *Nature 410*, 223−227.
12. Krebs, M. R., Morozova-Roche, L. A., Daniel, K., Robinson, C. V., and Dobson, C. M. (2004) Observation of sequence specificity in the seeding of protein amyloid fibrils, *Protein Sci. 13*, 1933−1938.
13. Hasegawa, K., Yamaguchi, I., Omata, S., Gejyo, F., and Naiki, H. (1999) Interaction between Aβ(1−42) and Aβ(1−40) in Alzheimer's β-amyloid fibril formation *in vitro*, *Biochemistry 38*, 15514−15521.
14. Kozhukh, G. V., Hagihara, Y., Kawakami, T., Hasegawa, K., Naiki, H., and Goto, Y. (2002) Investigation of a peptide responsible for amyloid fibril formation of β2-microglobulin by achromobacter protease I, *J. Biol. Chem. 277*, 1310−1315.
15. Yoshiike, Y., Chui, D. H., Akagi, T., Tanaka, N., and Takashima, A. (2003) Specific compositions of amyloid-β peptides as the determinant of toxic β-aggregation, *J. Biol. Chem. 278*, 23648−23655.
16. Fu, X., Korenaga, T., Fu, L., Xing, Y., Guo, Z., Matsushita, T., Hosokawa, M., Naiki, H., Baba, S., Kawata, Y., Ikeda, S., Ishihara, T., Mori, M., and Higuchi, K. (2004) Induction of AApoAII amyloidosis by various heterogeneous amyloid fibrils, *FEBS Lett. 563*, 179−184.
17. Takahashi, Y., Ueno, A., and Mihara, H. (2002) Amyloid architecture: Complementary assembly of heterogeneous combinations of three or four peptides into amyloid fibrils, *ChemBioChem 3*, 637−642.
18. Jarrett, J. T., and Lansbury, P. T., Jr. (1993) Seeding "one-dimensional crystallization" of amyloid: A pathogenic mechanism in Alzheimer's disease and scrapie? *Cell 73*, 1055−1058.
19. Blundell, T. L., Dodson, G. G., Hodgkin, D. M., and Merola, F. (1972) *Insulin*, 26th ed., pp 279−402.
20. Baker, E. N., Blundell, T. L., Cutfield, J. F., Cutfield, S. M., Dodson, E. J., Dodson, G. G., Hodgkin, D. M., Hubbard, R. E., Isaacs, N. W., and Reynolds, C. D. (1988) The structure of 2Zn pig insulin crystals at 1.5 Å resolution, *Philos. Trans. R. Soc. London, Ser. B 319*, 369−456.
21. Brange, J., Skelbaek-Pedersen, B., Langkjaer, L., Damgaard, U., Ege, H., Havelund, S., Heding, L. G., Jorgensen, K. H., Lykkeberg, J., Markussen, J., Pingel, M., and Rasmussen, E. (1987) The physicochemical and pharmaceutical aspects of insulin and insulin preparations, *Gelenics of Insulin*, Springer-Verlag, Berlin, Germany.
22. Waugh, D. F., Wilhelmson, D. F., Sackler, M. L., and Commerford, S. L. (1953) Studies of the nucleation and growth reactions of selected types of insulin fibrils, *J. Am. Chem. Soc. 75*, 2592−2600.
23. Waugh, D. F. (1946) A fibrous modification of insulin. I. The heat precipitate of insulin, *J. Am. Chem. Soc. 68*, 247−250.
24. Jansen, R., Dzwolak, W., and Winter, R. (2005) Amyloidogenic self-assembly of insulin aggregates probed by high-resolution atomic force microscopy, *Biophys. J. 88*, 1344−1353.
25. Ahmad, A., Millett, I. S., Doniach, S., Uversky, V. N., and Fink, A. L. (2004) Stimulation of insulin fibrillation by urea-induced intermediates, *J. Biol. Chem. 279*, 14999−15011.
26. Arora, A., Ha, C., and Park, C. B. (2004) Insulin amyloid fibrillation at above 100 °C: New insights into protein folding under extreme temperatures, *Protein Sci. 13*, 2429−2436.
27. Dzwolak, W., Smirnovas, V., Jansen, R., and Winter, R. (2004) Insulin forms amyloid in a strain-dependent manner: An FT-IR spectroscopic study, *Protein Sci. 13*, 1927−1932.
28. Jansen, R., Grudzielanek, S., Dzwolak, W., and Winter, R. (2004) High pressure promotes circularly shaped insulin amyloid, *J. Mol. Biol. 338*, 203−206.
29. Khurana, R., Ionescu-Zanetti, C., Pope, M., Li, J., Nielson, L., Ramirez-Alvarado, M., Regan, L., Fink, A. L., and Carter, S. A. (2003) A general model for amyloid fibril assembly based on morphological studies using atomic force microscopy, *Biophys. J. 85*, 1135−1144.
30. Ahmad, A., Millett, I. S., Doniach, S., Uversky, V. N., and Fink, A. L. (2003) Partially folded intermediates in insulin fibrillation, *Biochemistry 42*, 11404−11416.
31. Khurana, R., Ionescu-Zanetti, C., Pope, M., Li, J., Nielson, L., Ramirez-Alvarado, M., Regan, L., Fink, A. L., and Carter, S. A. (2003) A general model for amyloid fibril assembly based on morphological studies using atomic force microscopy, *Biophys. J. 85*, 1135−1144.
32. Jimenez, J. L., Nettleton, E. J., Bouchard, M., Robinson, C. V., Dobson, C. M., and Saibil, H. R. (2002) The protofilament structure of insulin amyloid fibrils, *Proc. Natl. Acad. Sci. U.S.A. 99*, 9196−9201.
33. Nielsen, L., Frokjaer, S., Carpenter, J. F., and Brange, J. (2001) Studies of the structure of insulin fibrils by Fourier transform infrared (FTIR) spectroscopy and electron microscopy, *J. Pharm. Sci. 90*, 29−37.
34. Nielsen, L., Frokjaer, S., Brange, J., Uversky, V. N., and Fink, A. L. (2001) Probing the mechanism of insulin fibril formation with insulin mutants, *Biochemistry 40*, 8397−8409.
35. Uversky, V. N., Garriques, L. N., Millett, I. S., Frokjaer, S., Brange, J., Doniach, S., and Fink, A. L. (2003) Prediction of the association state of insulin using spectral parameters, *J. Pharm. Sci. 92*, 847−858.
36. Petkova, A. T., Leapman, R. D., Guo, Z., Yau, W. M., Mattson, M. P., and Tycko, R. (2005) Self-propagating, molecular-level polymorphism in Alzheimer's β-amyloid fibrils, *Science 307*, 262−265.
37. Brange, J., Whittingham, J. L., Edwards, D. J., Youshang, Z., Wollmer, A., Brandenberg, D., Dodson, G. G., and Finch, J. (1997) Insulin, *Curr. Sci. 72*, 470−476.
38. Brange, J., Dodson, G. G., Edwards, D. J., Holden, P. H., and Whittingham, J. L. (1997) A model of insulin fibrils derived from the X-ray crystal structure of a monomeric insulin (despentapeptide insulin), *Proteins 27*, 507−516.
39. Nielsen, L., Khurana, R., Coats, A., Frokjaer, S., Brange, J., Vyas, S., Uversky, V. N., and Fink, A. L. (2001) Effect of environmental factors on the kinetics of insulin fibril formation: Elucidation of the molecular mechanism, *Biochemistry 40*, 6036−6046.
40. Porter, R. R. (1953) Partition chromatography of insulin and other proteins, *Biochem. J. 53*, 320−328.
41. Gill, S. C., and von Hippel, P. H. (1989) Calculation of protein extinction coefficients from amino acid sequence data, *Anal. Biochem. 182*, 319−326.
42. Oberg, K. A., and Fink, A. L. (1998) A new attenuated total reflectance Fourier transform infrared spectroscopy method for the study of proteins in solution, *Anal. Biochem. 256*, 92−106.
43. Seshadri, S., Khurana, R., and Fink, A. L. (1999) Fourier transform infrared spectroscopy in analysis of protein deposits, *Methods Enzymol. 309*, 559−576.
44. Sluzky, V., Klibanov, A. M., and Langer, R. (1992) Mechanism of insulin aggregation and stabilization in agitated aqueous solutions, *Biotechnol. Bioeng. 40*, 895−903.
45. Fink, A. L., Seshadri, S., Khurana, R., and Oberg, K. A. (1999) Determination of secondary structure in protein aggregates using attenuated total reflectance (ATR) FTIR, in *Infrared Analysis of Peptides and Proteins* (Singh, B. R., Ed.) pp 132−144, The American Chemical Society, Washington, DC.
46. Bryant, C., Strohl, M., Green, L. K., Long, H. B., Alter, L. A., Pekar, A. H., Chance, R. E., and Brems, D. N. (1992) Detection of an equilibrium intermediate in the folding of a monomeric insulin analog, *Biochemistry 31*, 5692−5698.
47. Millican, R. L., and Brems, D. N. (1994) Equilibrium intermediates in the denaturation of human insulin and two monomeric insulin analogs, *Biochemistry 33*, 1116−1124.
48. Bouchard, M., Zurdo, J., Nettleton, E. J., Dobson, C. M., and Robinson, C. V. (2000) Formation of insulin amyloid fibrils followed by FTIR simultaneously with CD and electron microscopy, *Protein Sci. 9*, 1960−1967.
49. Kihara, M., Chatani, E., Sakai, M., Hasegawa, K., Naiki, H., and Goto, Y. (2005) Seeding-dependent maturation of β2-microglobulin amyloid fibrils at neutral pH, *J. Biol. Chem.*
50. Borysik, A. J. H., Radford, S. E., and Ashcroft, A. E. (2004) Co-populated conformational ensembles of β2-microglobulin uncovered quantitatively by electrospray ionization mass spectrometry, *J. Biol. Chem. 279*, 27069−27077.
51. Ohhashi, Y., Hasegawa, K., Naiki, H., and Goto, Y. (2004) Optimum amyloid fibril formation of a peptide fragment suggests the amyloidogenic preference of β2-microglobulin under physiological conditions, *J. Biol. Chem. 279*, 10814−10821.
52. O'Nuallain, B., Williams, A. D., Westermark, P., and Wetzel, R. (2004) Seeding specificity in amyloid growth induced by heterologous fibrils, *J. Biol. Chem. 279*, 17490−17499.
53. Lundmark, K., Westermark, G. T., Olsen, A., and Westermark, P. (2005) Protein fibrils in nature can enhance amyloid protein A amyloidosis in mice: Cross-seeding as a disease mechanism, *Proc. Natl. Acad. Sci. U.S.A. 102*, 6098−6102.

54. Derkatch, I. L., Uptain, S. M., Outeiro, T. F., Krishnan, R., Lindquist, S. L., and Liebman, S. W. (2004) Effects of Q/N-rich, polyQ, and non-polyQ amyloids on the de novo formation of the [PSI$^+$] prion in yeast and aggregation of Sup35 *in vitro*, *Proc. Natl. Acad. Sci. U.S.A. 101*, 12934−12939.

55. Jones, E. M., and Surewicz, W. K. (2005) Fibril conformation as the basis of species- and strain-dependent seeding specificity of mammalian prion amyloids, *Cell 121*, 63−72.

BI051658Y